

Magnetostructural coupling and magnetocaloric effect in Ni–Mn–In

B. Li, W. J. Ren,^{a)} Q. Zhang, X. K. Lv, X. G. Liu, H. Meng, J. Li, D. Li, and Z. D. Zhang
Shenyang National Laboratory for Material Science, Institute of Metal Research, and International Centre for Material Physics, Chinese Academy of Sciences, 72 Wenhua Road, Shenyang 110016, People's Republic of China

(Received 9 September 2009; accepted 8 October 2009; published online 28 October 2009)

Magnetic-field-induced martensitic phase transition and the concomitant change of volume are investigated in Ni–Mn–In alloy. A well-defined linear relationship is found between the quantity characterizing magnetic degree of freedom and the thermal expansion on behalf of structural degree of freedom, which demonstrates the magnetostructural coupling. Within the exchange-inversion model, such a linear relationship is theoretically derived and the magnetostructural correlation is elucidated. The lattice-entropy change contributes about one half of the total entropy change, suggesting that the magnetostructural coupling plays an important role in the magnetocaloric effect of Ni–Mn–In alloy. © 2009 American Institute of Physics. [doi:10.1063/1.3257381]

In a magnetostructurally coupled system, a magnetic field can induce a remarkable structural change concomitant with a series of exotic properties, which results from the coupling between structural and magnetic degrees of freedom.^{1–3} Therefore, understanding the magnetostructural relationships in this kind of system is of vital importance both for unveiling the physics of the coupling between structural and magnetic degrees of freedom and for tailoring the functionalities of materials. As a typical magnetostructurally coupled system, metamagnetic shape-memory Ni–Mn–In alloy undergoes a magnetic-field-induced reverse martensitic transformation from antiferromagnetic (AF) martensite to ferromagnetic (FM) austenite, which has been extensively investigated because of its multifunctionality since discovered in 2004.^{4–11} Stresses over 100 MPa may be generated in a Co-doped Ni–Mn–In alloy under a moderate driving magnetic field, while in Ni–Mn–Ga, the generated stress is restricted to only several MPa for the rearrangement of martensitic twin variants induced by a comparative magnetic field, and a large driving magnetic field for the magnetic-field-induced martensitic transformation is required for generating large stresses.^{5,6,12} It suggests that Ni–Mn–In might be a more promising magnetic smart material than Ni–Mn–Ga. The magnetic-field-induced phase transition can also result in magnetic superelasticity,⁸ large magnetocaloric effect (MCE),⁹ large magnetoresistance, and giant magnetothermal conductivity.¹⁰ However, the correlation between the magnetic transition and the thermal expansion, and the influence of magnetostructural coupling on MCE have not been discussed yet. In this letter, we investigate magnetic-field-induced martensitic phase transition and the concomitant change of volume in Ni₅₀Mn₃₅In₁₅ alloy. We find a well-defined relationship between the quantities characterizing magnetic and structural degrees of freedom, which demonstrates the magnetostructural coupling. We further elucidate the magnetostructural correlation in terms of the exchange-inversion theory. The lattice-entropy change is determined by using the Debye model.

An alloy ingot of Ni–Mn–In with nominal composition of 50:35:15 was obtained by arc-melting appropriate amounts of the elements with purity of 99.9%. The ingot

was annealed at 900 °C for 48 h and quenched in ice water. X-ray diffraction (XRD) was performed on a D/max 2400 diffractometer (Rigaku) at room temperature. The XRD results indicate that the sample is single-phase with the 10 M martensitic structure.⁷ The elemental composition was determined to be Ni:Mn:In of 48.8:36.5:14.7 by an electronic probe microanalyzer (Shimadzu EPMA-1610). The magnetic properties were measured using a superconducting quantum inference device (SQUID) magnetometer (Quantum Design MPMS-XL). The temperature dependencies of zero-field-cooling (ZFC) and field-cooling (FC) magnetization were measured in such a procedure that the sample was first cooled at zero magnetic field to 220 K, and then measured at an applied magnetic field of 0.02 T from 220 to 370 K (ZFC) and back to 220 K (FC). Isothermal magnetization and demagnetization curves were measured during increasing temperature. The thermal expansion was measured using the standard strain-gauge technique connected with the SQUID.

The temperature dependencies of the ZFC and FC magnetizations under an applied magnetic field of 0.02 T are presented in Fig. 1. The alloy undergoes a transition from FM austenite to AF martensite at $T_M=281$ K, the reverse transition from AF martensite to FM austenite at $T_A=288$ K and the FM to paramagnetic transition at $T_C=316$ K. These characteristic temperatures are determined by the extremes of dM/dT . The noticeable thermal hysteresis of 7 K is a fingerprint of a first-order phase transition. The

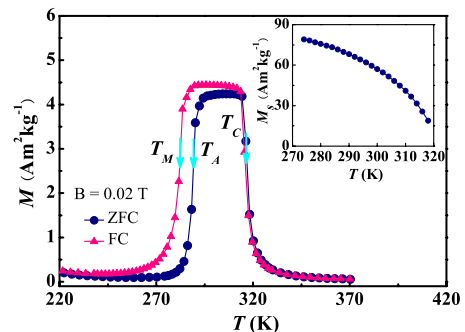


FIG. 1. (Color online) Temperature dependencies of the ZFC and FC magnetizations in a magnetic field of 0.02 T. The arrows mark the characteristic temperatures: $T_M=281$ K, $T_A=288$ K, and $T_C=316$ K, which are determined by the extremes of dM/dT . Inset: Temperature dependence of the spontaneous magnetization of the FM phase.

^{a)}Electronic mail: wjren@imr.ac.cn.

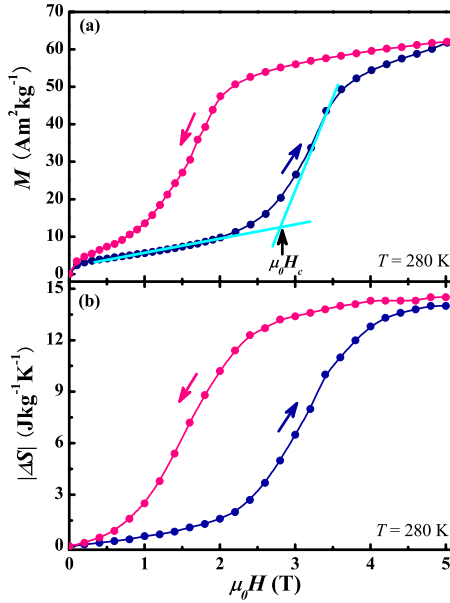


FIG. 2. (Color online) (a) Magnetic-field-induced martensitic phase transition and its reverse transition and (b) The magnetic-field dependencies of magnetic-entropy change at magnetization and demagnetization processes. The arrows mark the direction of the magnetic-field cycle 0 T–5 T–0 T.

isothermal magnetization and demagnetization processes at 280 K represented in Fig. 2(a) show that there is considerable magnetic hysteresis. The S-shaped curves indicate metamagnetic behavior: a FM to AF martensitic phase transition and the reverse AF to FM transition. The critical magnetic field $\mu_0 H_c$ for the martensitic phase transition is defined as the crossing point of the extrapolated straight lines from the regions where the magnetization increases slowly and subsequently increases strongly,⁸ as shown in Fig. 2(a). The magnetic-field dependencies of magnetic-entropy change are displayed in Fig. 2(b), which was calculated by the Maxwell relation. The magnetic-field-induced martensitic phase transition is the origin of the MCE so that the magnetic-field dependencies of magnetic-entropy change strongly resemble the isothermal magnetization and demagnetization curves.

In order to figure out how the magnetic degree of freedom correlates with the structural one, the thermal expansion and spontaneous magnetization are investigated. As presented in Fig. 3(a), the variation of thermal expansion $\Delta L/L_0$ with temperature for Ni–Mn–In exhibits a giant jump at the reverse martensitic phase transition, which originates basically from the change of the unit-cell volume at the reverse martensitic transition.⁷ The temperature dependence of

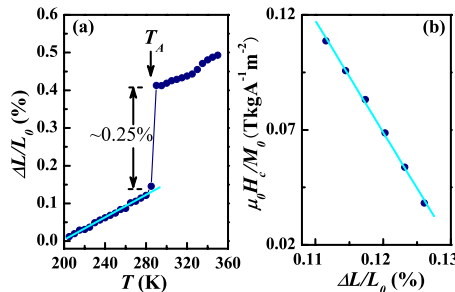


FIG. 3. (Color online) (a) Temperature dependence of the thermal expansion. The straight line corresponds to a linear fit to the temperature dependence of the thermal expansion. The arrow labels the reverse martensitic transition temperature. (b) The linear relationship between $\mu_0 H_c/M_0$ and $\Delta L/L_0$.

$\Delta L/L_0$ is linear in the martensite state,⁸ as shown by the straight-line fit in Fig. 3(a). The inset of Fig. 1 displays the variation of the spontaneous magnetization with temperature, which is obtained from Arrott plots.¹³ Considering the AF character of the martensitic phase, the spontaneous magnetization shown in the inset of Fig. 1 should be the sum of the magnetization of each sublattice. Simply, we assume there are two sublattices. Therefore, the magnetization of each sublattice should be one half of the spontaneous magnetization in the FM state, i.e., $M_0 = M_s/2$, where M_0 is the magnetization of one sublattice. Then, we try to plot $\mu_0 H_c/M_0$ versus $\Delta L/L_0$. It is exciting that there exists a good linear relationship, as shown in Fig. 3(b). Such a well-defined relationship correlating the magnetic degrees of freedom with structural degrees of freedom implies that there are some fundamental origins.

Due to the character of AF to FM transition, the exchange-inversion model is employed to study the transition. The exchange-inversion theory, proposed by Kittel,¹⁴ considers the dependence of the exchange interaction on the interatomic distance and describes quite well the AF to FM transitions in Mn_2Sb and in FeRh .^{15,16} In terms of this theory, the free energy including the exchange-interaction energy and the elastic energy of a volume V can be written as

$$F = \frac{1}{2}RV(a - a_T)^2 - \rho(a - a_c)VM_A M_B, \quad (1)$$

where a is the distance of magnetizations \mathbf{M}_A and \mathbf{M}_B of two sublattices, a_c denotes the critical value at which the interlattice exchange interaction changes sign, ρ is equal to $\partial\lambda/\partial a$ in which λ is the molecular-field constant involved \mathbf{M}_A and \mathbf{M}_B , R represents the appropriate elastic stiffness constant divided by a^2 and a_T stands for the equilibrium value of a at temperature T for the orientation $\mathbf{M}_A \perp \mathbf{M}_B$. Obviously, the free energy of the system is dependent on strain. The equilibrium value of a is given by

$$\left(\frac{\partial F}{\partial a}\right)_T = RV(a - a_T) - \rho VM_A M_B = 0. \quad (2)$$

Solving Eq. (2), one obtains

$$a = a_T + \frac{\rho}{R}(M_A M_B). \quad (3)$$

Combination of Eqs. (1) and (3) yields

$$\frac{F}{V} = -\frac{\rho^2}{2R}(M_A M_B)^2 - \rho(a_T - a_c)(M_A M_B). \quad (4)$$

Given $M_A = M_B = M_0$ and a transition driving force $2\mu_0 H_c M_0$, the energies of the two phases must be equal at the transition so that

$$\left(\frac{F}{V}\right)_{\text{AF}} + 2\mu_0 H_c M_0 = \left(\frac{F}{V}\right)_{\text{FM}}. \quad (5)$$

Substitution of Eq. (4) in Eq. (5) gives the solution for $\mu_0 H_c$

$$\mu_0 H_c = -\rho M_0(a_T - a_c). \quad (6)$$

The critical distance a_c is not dependent on temperature¹⁴ and, for an isotropic material, $(a_T - a_c)/a_c$ is proportional to the thermal expansion $\Delta L/L_0$. Therefore, it can be expected that $\mu_0 H_c/M_0$ is proportional to $\Delta L/L_0$.

From the temperature dependencies of the magnetization and the thermal expansion [see Figs. 1 and 3(a)], we can

conclude that a smaller distance between the sublattices facilitates the AF arrangement of the magnetic moments whereas a relatively larger distance is beneficial for the FM arrangement. The positive thermal-expansion coefficient for Ni₅₀Mn₃₅In₁₅ suggests that the AF state becomes less stabilized and the FM state can be much more easily induced by an applied magnetic field as the temperature increases. Just at the critical distance where $a_T = a_c$, the transition occurs. It is important to note that a_T , and not the actual distance a of the sublattices, enters the condition of exchange inversion.¹⁴ The critical magnetic field $\mu_0 H_c$ for the transition, by consequence, is determined by how much a_T deviates from a_c . Therefore, the coupling between the structural and the magnetic degrees of freedom can be demonstrated by Eq. (6).

A first-principles calculation suggests that the large spatial separation of Mn atoms ($>4 \text{ \AA}$) leads to Ruderman–Kittel–Kasuya–Yoshida (RKKY) exchange interaction in the $L2_1$ -type Ni–Mn–In alloy, which is mediated by conduction electrons.¹⁷ The RKKY exchange interaction is characterized by oscillatory behavior with the sign dependent on the relative position of magnetic moments. Given that the sign of exchange interaction is dependent on the interlattice distance in Ni–Mn–In, the exchange inversion provides evidence for the RKKY exchange interaction predicted by the first-principles calculation.

It is helpful to ascertain the individual contributions of the magnetic subsystem and the lattice subsystem to the total entropy change in this magnetostructurally coupled system because the so-called “magnetic-entropy change” obtained by the Maxwell relation represents the total entropy change for a first-order transition, mainly consisting of spin-entropy and lattice-entropy changes.^{18,19} The Debye theory gives the lattice entropy for one mole substance²⁰

$$S_L = -3Nk_B \ln \left[1 - \exp\left(-\frac{\Theta}{T}\right) \right] + 12Nk_B \left(\frac{T}{\Theta}\right)^3 \int_0^{\Theta/T} \frac{x^3 dx}{\exp(x) - 1}, \quad (7)$$

where N is the number of atoms per mole, k_B is the Boltzmann constant, and Θ is the Debye temperature. For a magnetostructurally coupled system, the lattice entropy is connected to the magnetic subsystem through the dependence of the Debye temperature Θ on the deformation^{21,22}

$$\Theta = \Theta_0(1 - \gamma\omega), \quad (8)$$

where Θ_0 , γ , and ω are the Debye temperature in absence of lattice deformation, the Grüneisen parameter and the volume change $\Delta V/V_0$, respectively. From the thermal-expansion jump of the reverse martensitic phase transition, ω was determined to be about 0.75% by supposing that the material is isotropic. Usually, γ is between 1 and 3.²³ The first-principles calculation suggests that γ is 2.405 for Heusler Ni–Mn–Sb alloy²⁴ and we adopt the same value for our Ni–Mn–In calculation. The martensite’s Debye temperature, as derived from Ref. 10, is 288 K. Combining Eqs. (7) and (8), we obtain the lattice-entropy change ΔS_L of the reverse transition to be about $6.6 \text{ J kg}^{-1} \text{ K}^{-1}$ at 280 K. This means that the lattice-entropy change would be about one half of the total entropy change [$14 \text{ J kg}^{-1} \text{ K}^{-1}$, see Fig. 2(b)] in Ni–Mn–In. The contribution of the lattice-entropy change to the total entropy change in Ni–Mn–In is very close to that in the $R_5(\text{Si}_{1-x}\text{Ge}_x)_4$ ($R = \text{Gd, Tb}$) systems, in which alloying or

hydrostatic pressure can change the order of transitions.^{2,25,26}

The calculation result tells us that the magnetostructural coupling plays an important role in the MCE of this alloy.

In conclusion, the magnetic degree of freedom and the structural one are coupled in the metamagnetic shape-memory material Ni–Mn–In. The intrinsic correlation between them is demonstrated by the relationship between $\mu_0 H_c/M_0$ and $\Delta L/L_0$. The lattice-entropy change accounts for about one half of the total entropy change, which suggests that the magnetostructural coupling plays an important role in the MCE of Ni–Mn–In alloy.

This work has been supported by the National Natural Science Foundation of China (Grant No. 50831006) and by the National Basic Research Program (Grant No. 2010CB934603) of China, Ministry of Science and Technology China.

¹A. Planes, L. Mañosa, and A. Saxena, *Magnetism and Structure in Functional Materials* (Springer, Berlin, 2005).

²K. A. Gschneidner, Jr., V. K. Pecharsky, and A. O. Tsokol, *Rep. Prog. Phys.* **68**, 1479 (2005).

³A. Asamitsu, Y. Morimoto, Y. Tomioka, T. Arima, and Y. Tokura, *Nature (London)* **373**, 407 (1995).

⁴Y. Sutou, Y. Imano, N. Koeda, T. Omori, R. Kainuma, K. Ishida, and K. Oikawa, *Appl. Phys. Lett.* **85**, 4358 (2004).

⁵R. Kainuma, Y. Imano, W. Ito, Y. Sutou, H. Morito, S. Okamoto, O. Kitakami, K. Oikawa, A. Fujita, T. Kanomata, and K. Ishida, *Nature (London)* **439**, 957 (2006).

⁶R. Kainuma, K. Oikawa, W. Ito, Y. Sutou, T. Kanomata, and K. Ishida, *J. Mater. Chem.* **18**, 1837 (2008).

⁷T. Krenke, M. Acet, E. F. Wassermann, X. Moya, L. Mañosa, and A. Planes, *Phys. Rev. B* **73**, 174413 (2006).

⁸T. Krenke, E. Duman, M. Acet, E. F. Wassermann, X. Moya, L. Mañosa, A. Planes, E. Suard, and B. Ouladdia, *Phys. Rev. B* **75**, 104414 (2007).

⁹X. X. Zhang, B. Zhang, S. Y. Yu, Z. H. Liu, W. J. Xu, G. D. Liu, J. L. Chen, Z. X. Cao, and G. H. Wu, *Phys. Rev. B* **76**, 132403 (2007).

¹⁰B. Zhang, X. X. Zhang, S. Y. Yu, J. L. Chen, Z. X. Cao, and G. H. Wu, *Appl. Phys. Lett.* **91**, 012510 (2007).

¹¹A. Planes, L. Mañosa, and M. Acet, *J. Phys.: Condens. Matter* **21**, 233201 (2009).

¹²P. J. Webster, K. R. A. Ziebeck, S. L. Town, and M. S. Peak, *Philos. Mag. B* **49**, 295 (1984).

¹³A. Arrott, *Phys. Rev.* **108**, 1394 (1957).

¹⁴C. Kittel, *Phys. Rev.* **120**, 335 (1960).

¹⁵W. H. Cloud, T. A. Bither, and T. J. Swoboda, *J. Appl. Phys.* **32**, S55 (1961); T. A. Bither, P. H. L. Walter, W. H. Cloud, T. J. Swoboda, and P. E. Bierstedt, *ibid.* **33**, 1346 (1962); H. S. Jarrett, *Phys. Rev.* **134**, A942 (1964).

¹⁶P. H. L. Walter, *J. Appl. Phys.* **35**, 938 (1964); J. S. Kouvel, *ibid.* **37**, 1257 (1966); J. B. McKinnon, D. Melville, and E. W. Lee, *J. Phys. C* **3**, S46 (1970).

¹⁷E. Şaşıoğlu, L. M. Sandratskii, and P. Bruno, *Phys. Rev. B* **77**, 064417 (2008).

¹⁸S. Gama, A. A. Coelho, A. de Campos, A. M. G. Carvalho, and F. C. G. Gandraf, *Phys. Rev. Lett.* **93**, 237202 (2004).

¹⁹V. K. Pecharsky, A. P. Holm, K. A. Gschneidner, Jr., and R. Rink, *Phys. Rev. Lett.* **91**, 197204 (2003).

²⁰P. Debye, *Ann. Phys.* **39**, 789 (1912).

²¹P. J. von Ranke, N. A. de Oliveira, C. Mello, A. M. G. Carvalho, and S. Gama, *Phys. Rev. B* **71**, 054410 (2005).

²²G. J. Liu, J. R. Sun, J. Lin, Y. W. Xie, T. Y. Zhao, H. W. Zhang, and B. G. Shen, *Appl. Phys. Lett.* **88**, 212505 (2006).

²³C. Kittel, *Introduction to Solid State Physics*, 5th ed. (Wiley, New York, 1976).

²⁴A. Pugaczowa-Michalska, *Solid State Commun.* **140**, 251 (2006).

²⁵L. Morellon, Z. Arnold, C. Magen, C. Ritter, O. Prokhnenko, Y. Skokhod, P. A. Algarabel, M. R. Ibarra, and J. Kamarad, *Phys. Rev. Lett.* **93**, 137201 (2004).

²⁶D. Haskel, Y. B. Lee, B. N. Harmon, Z. Islam, J. C. Lang, G. Srajer, Ya. Mudryk, K. A. Gschneidner, Jr., and V. K. Pecharsky, *Phys. Rev. Lett.* **98**, 247205 (2007).